บทความวิจัย

# COMPARISON OF REMOTE SENSING TECHNIQUES FOR LAND USE CLASSIFICATION IN PATTANI BAY, THAILAND

Uten Thongtip*

[1*]Department of Geographical Technology, Faculty of Humanities and Social Sciences
Phranakhon Rajabhat University, Bangkok, 10220.

*E-mail: tane_geog@hotmail.com

Received: 2018-05-14
Revised: 2019-01-20
Accepted: 2019-01-30

## ABSTRACT

In Thailand the land use has been changing, every day new developments (urban, industrial, commercial and agricultural) are emerging. The purpose of this work is to develop the land use of Pattani Bay a sub-wetland of the Thailand watershed that is an important natural resource to Pattani Province. Remote sensing techniques can be used to assess several water quality parameters and also for land use classifications. For this work the ERDAS Imagine 2014 computer software will be used to develop a land use classification using LANDSAT-8 images. The generated land use classification will be compared with a land use generated using ArcGIS 10.5, to decide which method provides better land use classification. The accuracy of each of the derived classification products was assessed in several ways, after which different product accuracies were compared using statistical means with STATISTICA 13.

After used ERDAS to perform the classification, significant data has been obtained using a Minimum Distance Supervised Classification method. Correction methods need to be performed for shadows. Land use classification is more detailed using remote sensing tools such as ERDAS software than the ArcGIS. Also land use classification using ERDAS, can be performed faster and with more precision, after you have your training samples. Using the obtained results from ERDAS and ArcGIS for land use classification can help to perform a more accurate classification. To perform

a better classification of this area using ERDAS, it is recommended to use the Modeler Tool, to correct the errors and be more accurate.

**Keywords**: Comparison, Remote Sensing Techniques, Land Use Classification

## Introduction

Remote Sensing (RS) has been used to classify and map land use changes with different techniques and data sets. LANDSAT images in particular have served a great deal in the classification of different landscape components at a larger scale (Ozesmi & Bauer, 2002). Recently several change detection techniques have been developed that make use of remotely sensed images. A variety of change detection techniques and algorithms have been developed and reviewed for their advantages and disadvantages. Among these Unsupervised Classification or Clustering, Supervised Classification, PCA, Hybrid Classification and Fuzzy Classification are the most commonly applied techniques used in classification (Lu et al., 2004), (Rundquist et al., 2001), (Zhang et al., 2000).

The Operational Land Imager (OLI) and Thermal Infrared Sensor (TIRS) are instruments onboard the LANDSAT-8 satellite, which was launched in February of 2013. The satellite collects images of the Earth with a 16 day repeat cycle, referenced to the Worldwide Reference System-2. The satellite's acquisitions are in an 8-day offset to LANDSAT-7. The approximate scene size is 170 km. north-south by 183 km. east-west (106 mi by 114 mi). Data collected by the instruments onboard the satellite are available to download at no charge from EarthExplorer, GloVis, or the LANDSATLook Viewer within 24 hours of acquisition (U.S. Geological Survey, 2017).

Pattani Bay is a semi-enclosed reservoir which connects to the Yaring River and its branches and the Gulf of Thailand. It is one of the important water bodies in southern Thailand which supply natural resources (Ruangchuay et al., 2007). The study area was selected for change detection because of being subjected to urbanization, sewage discharges without treatment, active water and soil erosion, over grazing, cutting of trees, non-existence of any cooperative communal structure and reduced livelihood opportunities (Pirut, 2015). Along with these, rapid discharge of pesticide residues and poultry discharge in the streams is also one of the major concerns faced by the Pattani Bay due to the rapidly increasing agricultural activities and number of poultry farms in the study area. The rapid urban development taking place in the study area has led to environmental problems as well, encompassing, fragmentation of aquatic habitats, soil erosion, and water pollution due to deforestation and discharge of municipal garbage and industrial waste (Erftemeijer & Bualuang, 2015).

**Objectives**

1. Use remote sensing techniques to identify the land use of Pattani Bay in Thailand.

2. Compare the distribution of land use areas to identify which is the most predominant in the Pattani Bay (Agriculture, Bare soil/rocks, Settlements, Vegetation and Water.)

3. Compare the land use classification data generated by ERDAS IMAGINE 2014 vs. the data generated by using ArcGIS 10.5.

**Literature Review**

1. LANDAT-8

The LANDAT-8 instruments, Operational Land Imager (OLI) and Thermal Infrared Sensor (TIRS), represent an evolutionary advance in technology. OLI builds upon LANDAT heritage and technologies demonstrated by the ALI. As such, OLI is a push-broom sensor with a four-mirror telescope and uses 12-bit quantization. The OLI collects 30-meter data for visible, near infrared, and short wave infrared spectral bands as well as provides for a 15 meter panchromatic band. New with OLI is the addition of a 30-meter-deep blue Coastal Aerosol band (Band 1) for coastal water and aerosol studies and a 30 meter Cirrus band (Band 9) for cirrus cloud detection. Additionally, the bandwidth has been refined (narrowed) for six of the heritage bands (NASA, 2017).

The TIRS instrument collects data for two narrow spectral bands in the thermal region, formerly covered on previous LANDAT instruments by one wide spectral band. Although TIRS is a separate instrument, the 100 meter TIRS data are registered to the OLI data in order to create radiometrically, geometrically, and terrain-corrected 12-bit data products (NASA, 2017).

These sensors both provide improved SNR radiometric performance quantized over a 12-bit dynamic range. This translates into 4,096 potential grey levels in an image compared with only 256 grey levels in previous 8-bit instruments. Additionally, improved signal-to-noise performance enables better characterization of land cover state and condition (U.S. Geological Survey, 2017).

In addition to Table 1, Figure 1 compares LANDAT-8 spectral bands and wavelength to that of LANDAT-7 ETM+. The OLI sensor, which has a five-year design life, is similar in design to the Advanced Land Imager (ALI) that was included on EO-1, and represents a significant technological advancement over LANDSAT-7's Enhanced Thematic Mapper Plus (ETM+) sensor. Instruments on earlier Landsat satellites employed oscillating mirrors to sweep the detectors' field of view across the swath width ("whiskbroom"), but OLI instead uses long linear detector arrays with thousands of detectors per spectral band. Detectors aligned across the instrument focal planes collect imagery in a "push broom" manner resulting in a more sensitive instrument with fewer moving parts. OLI has a four-mirror telescope and data generated by OLI are quantized to 12 bits, compared to the 8-bit data produced by the TM & ETM+ sensor (U.S. Geological Survey, 2017).

**Table 1** OLI and TIRS Spectral Bands Compared to ETM+ Spectral Bands

| LANDSAT-7 ETM+ | | | | LANDSAT-8 OLI and TIRS | | | |
|---|---|---|---|---|---|---|---|
| Band | Name | Resolution (m.) | Spectrum (μm.) | Band | Name | Resolution (m.) | Spectrum (μm.) |
| 1 | Blue | 30 | 0.441 - 0.514 | 1 | Coastal/Aerosol | 30 | 0.435 - 0.451 |
| 2 | Green | 30 | 0.519 - 0.601 | 2 | Blue | 30 | 0.452 - 0.512 |
| 3 | Red | 30 | 0.631 - 0.692 | 3 | Green | 30 | 0.533 - 0.590 |
| 4 | NIR | 30 | 0.772 - 0.898 | 4 | Red | 30 | 0.636 - 0.673 |
| 5 | SWIR-1 | 30 | 1.547 - 1.749 | 5 | NIR | 30 | 0.845 - 0.885 |
| 6 | TIR | 60 | 10.31 - 12.36 | 6 | SWIR-1 | 30 | 1.566 - 1.651 |
| 7 | SWIR-2 | 30 | 2.064 - 2.345 | 7 | SWIR-1 | 30 | 2.107 - 2.294 |
| 8 | Pan | 15 | 0.515 - 0.896 | 8 | Pan | 15 | 0.503 - 0.676 |
| | | | | 9 | Cirrus | 30 | 1.363 - 1.384 |
| | | | | 10 | TIR-1 | 100 | 10.600 - 11.190 |
| | | | | 11 | TIR-2 | 100 | 11.500 - 12.510 |

**Source**: U.S. Geological Survey. (2017)

The OLI sensor collects image data for nine shortwave spectral bands over a 190 km. swath with a 30 m. spatial resolution for all bands except the 15 m. panchromatic band. The widths of several OLI bands are refined to avoid atmospheric absorption features within ETM+ bands. The biggest change occurs in OLI band 5 (0.845-0.885 µm.) to exclude a water vapor absorption feature at 0.825 µm. in the middle of the ETM+ near infrared band (band 4; 00.772-0.898 µm.). The OLI panchromatic band, band 8, is also narrower relative to the ETM+ panchromatic band to create greater contrast between vegetated areas and land without vegetation cover. OLI also has two new bands in addition to the legacy LANDSAT bands (1-5, 7, and Pan). The Coastal /Aerosol band (band 1; 0.435-0.451 µm.), principally for ocean color observations, is similar to ALI's band 1', and the new Cirrus band (band 9; 1.363-1.384 µm.) aids in detection of thin clouds comprised of ice crystals (cirrus clouds will appear bright while most land surfaces will appear dark through an otherwise cloud-free atmospheres containing water vapor).

OLI has stringent radiometric performance requirements and is required to produce data calibrated to an uncertainty of less than 5% in terms of absolute, at-aperture spectral radiance and to an uncertainty of less than 3% in terms of top-of-atmosphere spectral reflectance for each of the spectral bands in Table 1. These values are comparable to the uncertainties achieved by ETM+ calibration (U.S. Geological Survey, 2017)

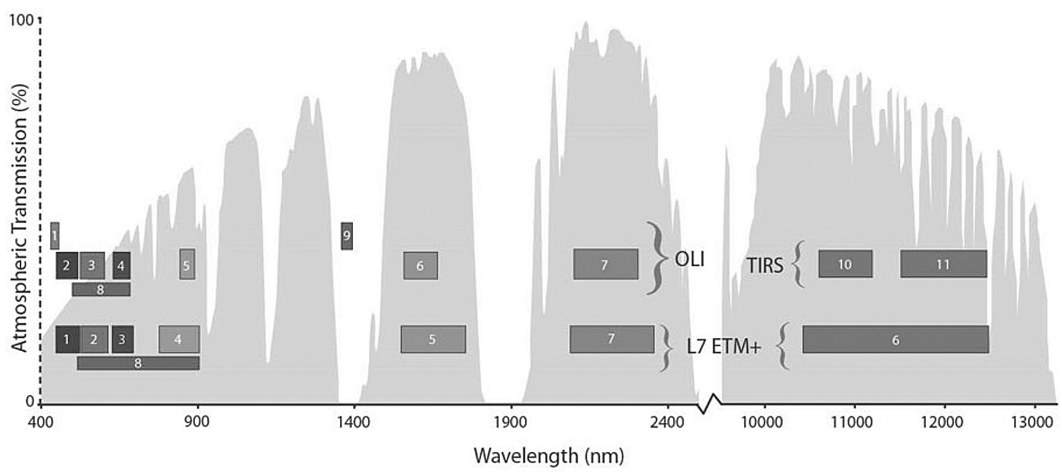


Figure 1 LANDSAT-8 Spectral Bands and Wavelengths compared to LANDSAT-7 ETM+

Source: U.S. Geological Survey. (2017)

2. Land Use Classification

The land use classification system presented in this report (Table 2) includes only the more generalized first and second levels. The system satisfies the three major attributes of the classification process as outlined by Grigg (1965): (1) it gives names to categories by simply using accepted terminology; (2) it enables information to be transmitted; and (3) it allows inductive generalizations to be made. The classification system is capable of further refinement on the basis of more extended and varied use. At the more generalized levels it should meet the principal objective of providing a land use classification system for use in land use planning and management activities. Attainment of the more fundamental and long-range objective of providing a standardized system of land use classification for national and regional studies will depend on the improvement that should result from widespread use of the system (Anderson et al., 1976).

**Table 2** Land Use Classification System for Use with Remote Sensor Data

| level 1 | level 2 |
|---|---|
| 1 Urban or built-up land | 11 Residential |
| | 12 Commercial and services |
| | 13 Industrial |
| | 14 Transportation |
| | 15 Industrial and commercial complexes |
| | 16 Mixed urban or built-up land |
| | 17 Other urban or built-up land |
| 2 Agriculture land | 21 Cropland and pasture |
| | 22 Orchards: groves, vineyards, nurseries, and ornamental horticulture areas |
| | 23 Confined feeding operations |
| | 24 Other agricultural land |
| 3 Rangeland | 31 Herbaceous rangeland |
| | 32 Shrub and brush rangeland |
| | 33 Mixed rangeland |
| 4 Forest land | 41 Deciduous forest land |
| | 42 Evergreen forest land |
| | 43 Mixed forest land |
| 5 Water | 51 Streams and canals |
| | 52 Lakes |
| | 53 bays and estuaries |
| 6 Wetland | 61 Forested wetland |
| | 62 Non forested wetland |
| 7 Barren land | 71 Dry salt flats |
| | 72 Beaches |
| | 73 Sandy areas other than beaches |
| | 74 Transitional areas |
| | 75 Mixed barren land |
| 8 Tundra | 81 Shurb and brush tundra |
| | 82 Herbaceous tundra |
| | 83 Mixed tundra |
| 9 Perennial snow and ice | 91 Perennial snowfield |
| | 92 Glaciers |

**Source:** Anderson et al. (1976)

3. Supervised and Unsupervised Classification

Classification is the process of sorting pixels into a finite number of individual classes, or categories, of data based on their data file values. If a pixel satisfies a certain set of criteria, then the pixel is assigned to the class that corresponds to that criterion. Supervised Classification is more closely controlled by you than Unsupervised Classification. In this process, you select pixels that represent patterns you recognize or can identify with help from other sources. Knowledge of the data, the classes desired, and the algorithm to be used is required before you begin selecting training samples. By identifying patterns in the imagery, you can "train" the computer system to identify pixels with similar characteristics. By setting priorities to these classes, you supervise the classification of pixels as they are assigned to a class value. If the classification is accurate, then each resulting class corresponds to a pattern that you originally identified. Unsupervised Classification is more computer-automated. It allows you to specify parameters that the computer uses as guidelines to uncover statistical patterns in the data (Intergraph Corporation, 2013).

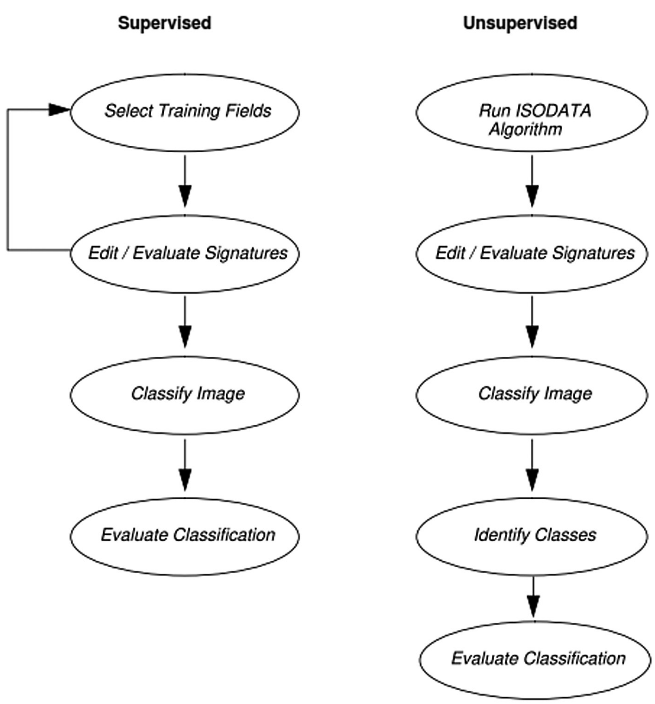


Figure 2: Supervised and Unsupervised Classification

Source: Intergraph Corporation, (2013)

3.1 ISODATA and K-Means Classification

Today several different unsupervised classification algorithms are commonly used in remote sensing. The two most frequently used algorithms are the K-mean and the ISODATA clustering algorithm. Both of these algorithms are iterative procedures. In general, both of them assign first an arbitrary initial cluster vector. The second step classifies each pixel to the closest cluster. In the third step the new cluster mean vectors are calculated based on all the pixels in one cluster. The second and third steps are repeated until the “change” between the iteration is small. The “change” can be defined in several different ways, either by measuring the distances the mean cluster vector have changed from one iteration to another or by the percentage of pixels that have changed between iterations.

The ISODATA algorithm has some further refinements by splitting and merging of clusters (Jensen, 1996). Clusters are merged if either the number of members (pixel) in a cluster is less than a certain threshold or if the centers of two clusters are closer than a certain threshold. Clusters are split into two different clusters if the cluster standard deviation exceeds a predefined value and the number of members (pixels) is twice the threshold for the minimum number of members. The ISODATA algorithm is similar to the k-means algorithm with the distinct difference that the ISODATA algorithm allows for different number of clusters while the k-means assumes that the number of clusters is known a priori. The objective of the k-means algorithm is to minimize the within cluster variability. The objective function (which is to be minimized) is the sums of squares distances (errors) between each pixel and its assigned cluster center.

K-means (just as the ISODATA algorithm) is very sensitive to initial starting values. For two classifications with different initial values and resulting different classification one could choose the classification with the smallest MSE (since this is the objective function to be minimized). However, as we show later, for two different initial values the differences in respects to the MSE are often very small while the classifications are very different. Visually it is often not clear that the classification with the smaller MSE is truly the better classification. From a statistical viewpoint, the clusters obtained by k-mean can be interpreted as the Maximum Likelihood Estimates (MLE) for the cluster means if we assume that each cluster comes from a spherical Normal distribution with different means but identical variance (and zero covariance).

This touch upon a general disadvantage of the K-Means algorithm (and similarly the ISODATA algorithm): K-Means works best for images with clusters that are spherical and that have the same variance (Lillesand & Kiefer, 2000).

This is often not true for remote sensing images. For example, a cluster with "desert" pixels is compact/circular. A "forest" cluster, however, is usually more or less elongated/oval with a much larger variability compared to the "desert" cluster. While the "desert" cluster is usually very well detected by the k-means algorithm as one distinct cluster, the "forest" cluster is often split up into several smaller clusters. The way the "forest" cluster is split up can vary quite a bit for different starting values and is thus arbitrary (Lillesand & Kiefer, 2000).

3.2 Minimum Distance Classification

First, we will learn about the theoretical background of the Minimum Distance Classification using a simplified example. The simplest case is the 2-dimensional spectral feature space. You can see it in Figure 3. The axes correspond to the image spectral bands. Each pixel of the satellite image corresponds to a point in the feature space. The figure shows three classes, that are in red, green and blue points. The red point cloud overlaps with the green and blue ones. There is also a black point cloud that does not belong to any class. After the image is classified these points will correspond to classified pixels (Pavel, 2017).

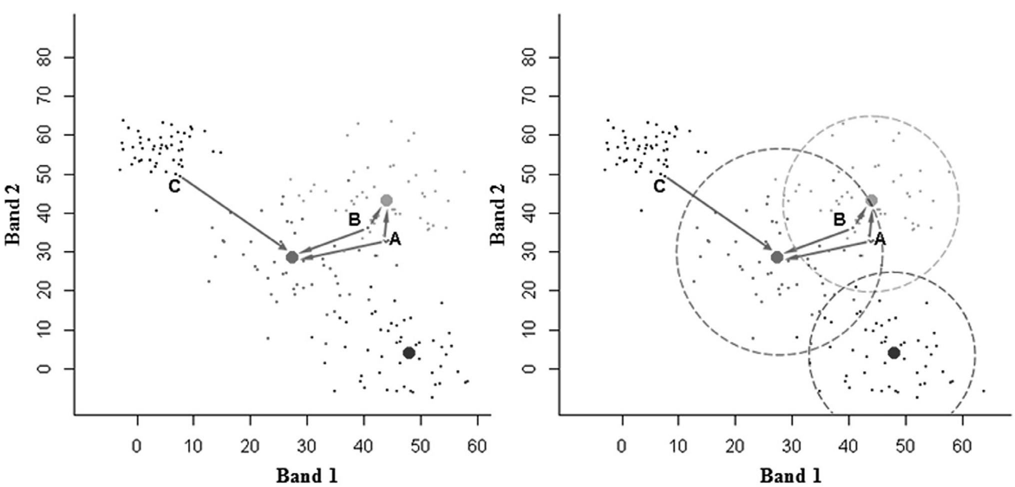


Figure 3: Minimum Distance Classification

Source: Pavel, (2017)

Figure 3 on the left shows a situation where the classification does not include the possibility of unclassified pixels. And figure 3 on the right, on the contrary, a case with unclassified pixels in the results of the classification. The grey arrows show the distance from the green point A and the red point B to the centers of green and red classes. We see that both points are closer to the green class center. Therefore points A and B will be classified by the minimum distance to the green class. Here we see the principle of determining membership in the class and the source of errors in the classification. But the number of errors will be less than when we limit the classes to rectangles, as in the classification by the parallelepiped algorithm. That is why when brightness values of classes overlap it is recommended to use a minimum distance algorithm, rather than a parallelogram algorithm (Pavel, 2017).

If we assume the presence of unclassified pixels, the algorithm of the Minimum Distance gets slightly more complicated. Figure 3 show a black point marked as C. The closest class center to it is the center of the red class. To exclude this point from classification procedure, you need to limit the search range around the class centers. For this, set the maximum permissible distance from the center of the class. Figure 3 on the right shows an example of this. Maximum Distances from the centers of the class that limit the search radius are marked with dashed circles. Without this restriction, most black points would be assigned to the red class, and some-to green (Figure. 3, left). And with the restriction (Figure. 3, on the right) they will remain unclassified (Pavel, 2017).

You can apply a search restriction of the same value to all classes. This is the case when all classes have a similar spread of values. And if the classes have a very different spread of values, then it is necessary to set for each class its own size of the search radius. This more complex case is shown in Figures 1 on the right when a greater distance from the center of the class is defined for the red class than for the blue or the green one (Pavel, 2017).

**Study Area**

Located in the Pattani Bay, Thailand, on the Pattani Province fringe, the study area (Figure 4) is about 76.91 $Km^2$ in size.

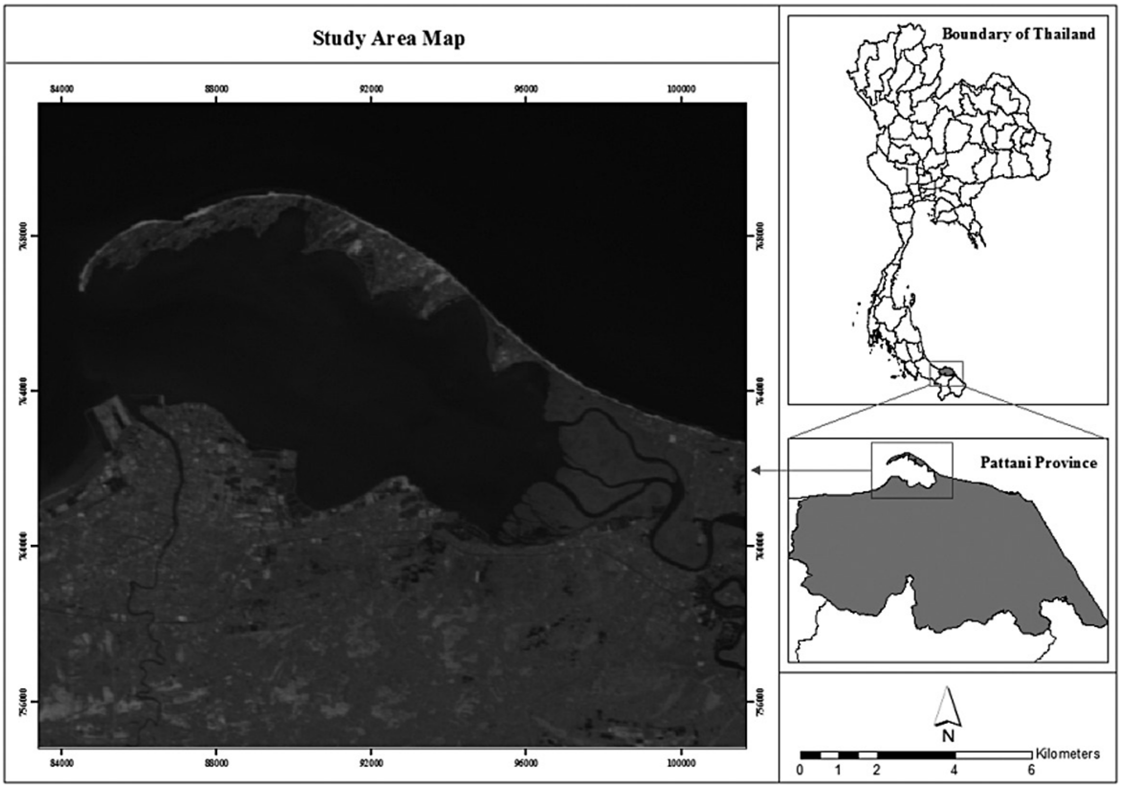


Figure 4 Study Area Map

## Methods

Initially, a LANDAT-8 images of the Pattani Bay was pre-processed and then classified in several ways using ERDAS IMAGINE 2014. Post-classification, a decision support system based on expert-knowledge was used to update the classification products according to existing land-use databases using ArcGIS 10.5. The accuracy of each of the derived classification products was assessed in several ways, after which different product accuracies were compared using statistical means with STATISTICA 13. Figure 5 presents a flowchart of the work.

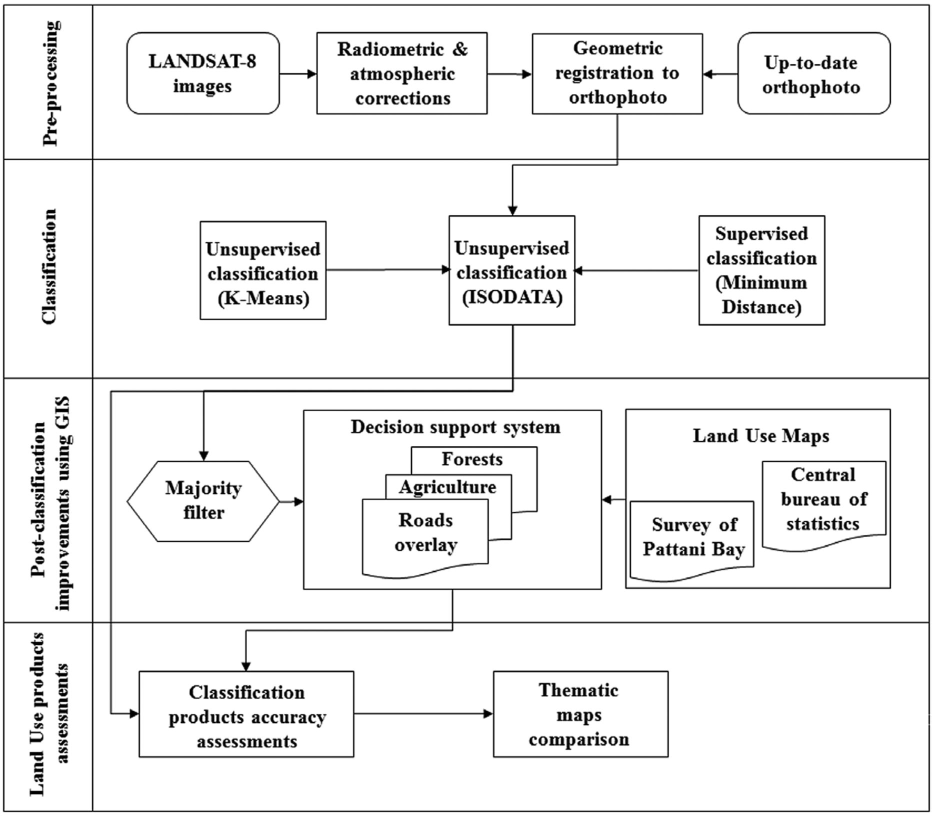


Figure 5 Research Flowchart

For this research, true color images of LANDAT-8 will be used to identify the study area. Remote sensing techniques using ERDAS software to process LANDAT-8 images for the area of interest will be used (Intergraph Corporation, 2013). DEM (Digital Elevation Models) will be used to delineate the catchments area of the subbasing (Río Jauca). ArcGIS (ESRI, 2015) will be used to process the data obtained from DEM's, (Figure 5). The remote sensor to be used is LANDAT-8 which produces 15-meter black-and-white (panchromatic) and 15-meter multispectral (red, blue, green, near infrared) imagery that can be combined in a variety of ways to accommodate a wide range of high-resolution imagery applications using supervised classification. The LANDAT-8 images: LC08_L1TP_128055_20170307_20170316_01_T1 and LC08_TP_127056_20160414_20170326_01_T1 were obtained from the U.S. Geological Survey. A mosaic was obtained from the two images and then a mask created to work in the study area.

Classification for this study, Level 1 of the Anderson classification system was used (Anderson et al., 1976). This classification system is designed to mainly rely on remote sensing; therefore only land-use and land cover types identifiable by remote sensing are used as the basis for organizing this classification. Level 1 of the Anderson classification system is recommended for use with Landsat resolution data. Although this classification scheme is coarse, it eliminates misclassification errors and makes delineation of categories more substantial (Zomeni & Pantis, 2008 and Mallinis et al., 2011). The different land-uses and land-covers included in the five classes used by this study are detailed in Table 3.

**Table 3** Land use classification system for use with LANDSAT-8 data

| Sr. No. | Class Name | Description |
|---|---|---|
| 1 | Agriculture | Crop fields and fallow lands |
| 2 | Settlements | Residential, commercial, industrial, transportation, roads, mixed urban |
| 3 | Bare soil/rock | Land areas of exposed soil and barren area influenced by human influence |
| 4 | Vegetation | Deciduous forest land, evergreen forest land and mixed forest land |
| 5 | Water | River, open water, lakes and ponds |

Source: Anderson et al. (1976)

Two Unsupervised Classifications were generated using ERDAS, one using ISODATA and the other using a K-Means method. Several Supervised Classifications were generated, to select the most appropriate. For this classification approximately 200 training samples were obtained from a visit to the area of study (Table 4) (Figure 7), using a Global Position System (GPS) to collect the data. The software used for this study is: ERDAS, ArcGIS and STATISTICA.

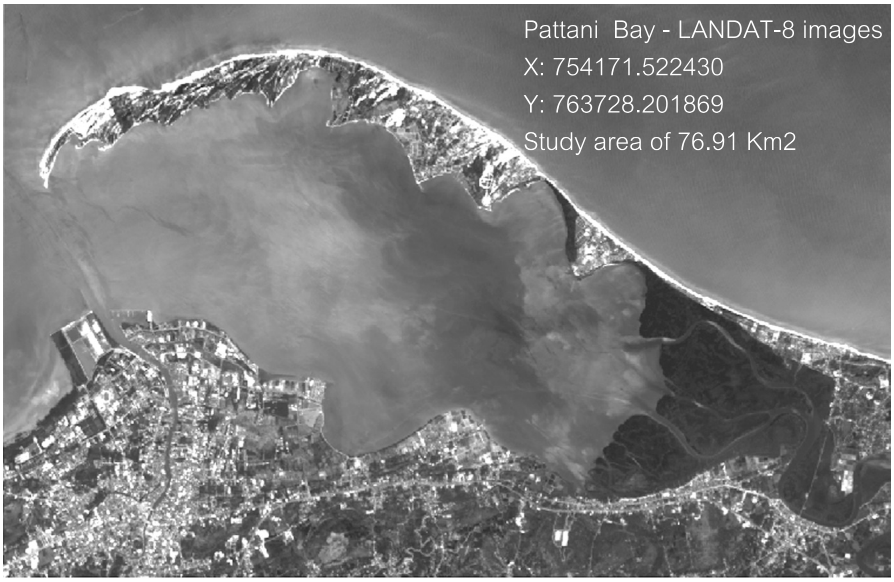


**Figure 6**: Pattani Bay, LANDAT-8

**Table 4** Training Samples Description (Example)

| Site | | UTM Grid Coordinate and Sampling | |
|---|---|---|---|
| Id | Name | X | Y |
| Sampling | | | |
| 1. | Agriculture | 757600 | 758900 |
| Point | | | 40 |
| 2. | Bare soil/rocks | 746800 | 766800 |
| Point | | | 40 |
| 3. | Settlements | 747500 | 759000 |
| Point | | | 40 |
| 4. | Vegetation | 760200 | 761300 |
| Point | | | 40 |
| 5. | Water | 748500 | 763100 |
| Point | | | 40 |

**Figure 7** Area of Interest (AOI) Selection Using Training Samples Areas

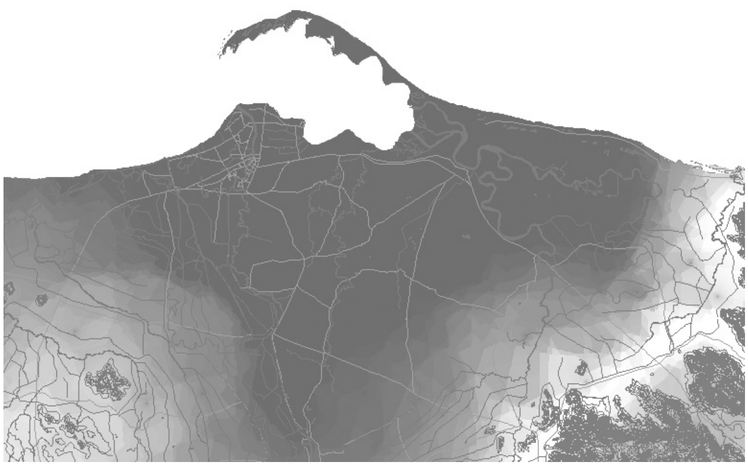

**Figure 8** Pattani Bay Delineation Using the Water Modeling System (WMS)

## Results and Discussions

Unsupervised Classification (Figures 9 and 10) Performing this classification generated some errors, especially in the forest and agricultural land. This classification was a significant tool to continue with the Supervised Classification. In this classification the most common errors were observed between the agriculture, pasture and forest classes, also errors were found in the urban area, that were in some areas classified as clouds. These errors can be corrected using atmospheric corrections, for clouds and shadows in the original image of LANDAT-8.

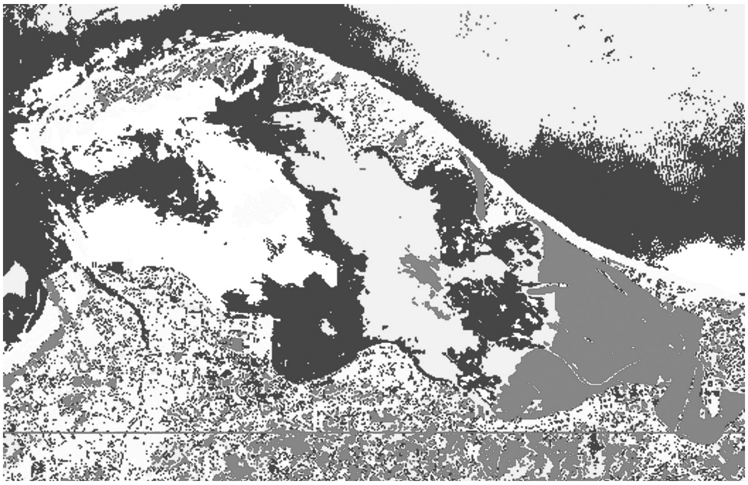

**Figure 9** Unsupervised Classification: K-Means Method

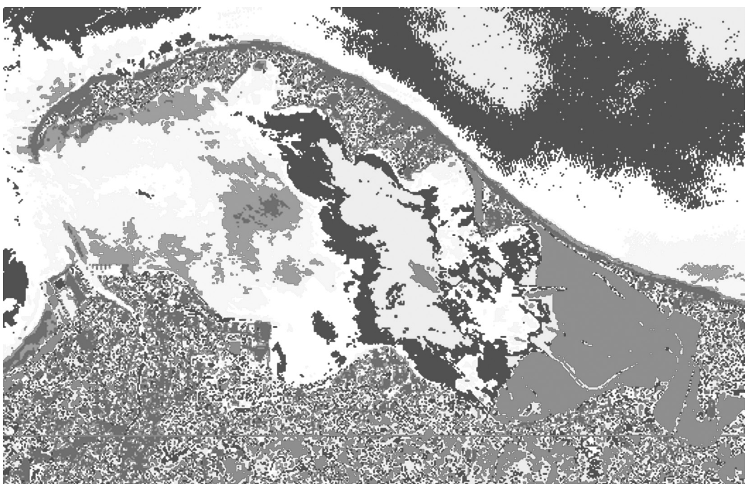

**Figure 10** Unsupervised Classification: Isodata Method

Supervised Classification (Figure 11) After generated eight different Supervised Classifications using different parameters such as number of classes and parametric methods; Minimum Distance, It was found that Minimum Distance Classification generated a better classification than Maximum Likelihood Classification. In the Supervised Classification the most common errors were found in the classification of pasture and forest, in some areas the wavelength of these elements was confused, this can be due to the high intensity of green land cover of the area and the intensity of forest in the watershed.

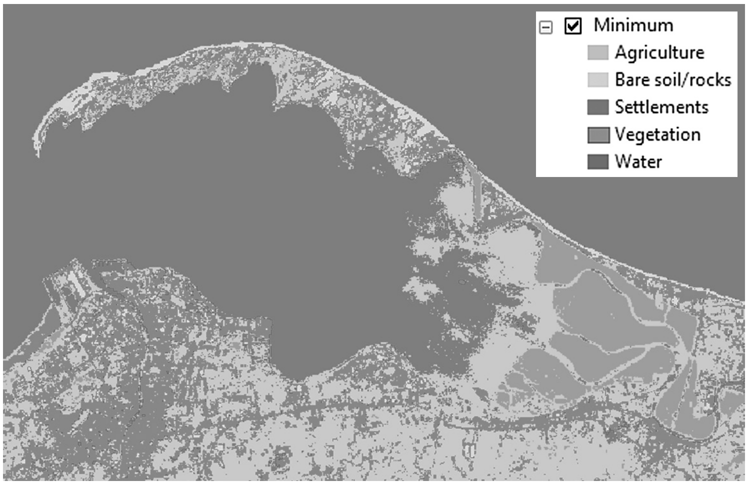


**Figure 11** Supervised Classification Minimum Distance Method

ArcGIS Classification in the land use classification generated using ArcGIS tools; the distribution of land use is the following: the predominant land use of the area is agriculture, followed by settlements, followed by vegetation, and a small portion of the bay composed a bare soil/rocks area. In this classification the rangeland area that is located in the center of the bay cannot be observed.

The classified LU map of Pattani Bay of years 2016 is given in Figure 12. The achieved overall classification accuracy 96.24% and overall kappa statistics were 0.9181 respectively for the classification 2016 images. According to Lea & Curtis (2010), accuracy assessment reporting requires the overall classification accuracy above 90% and kappa statistics above 0.9 which were successfully achieved in the present research.

The classification results for 2016 are summarized in Table 5. Percentage of classes based on these results show the land use practices observed in bay area during 2016.

**Table 5** Land Use Classes and Areas in Square Kilometers

| Land Use Classes | 2016 | |
|---|---|---|
| | Area ($km^2$) | % |
| Agriculture | 28.48 | 37.04 |
| Bare soil/rocks | 1.91 | 2.48 |
| Settlements | 19.96 | 25.95 |
| Vegetation | 21.59 | 28.07 |
| Water | 4.97 | 6.46 |

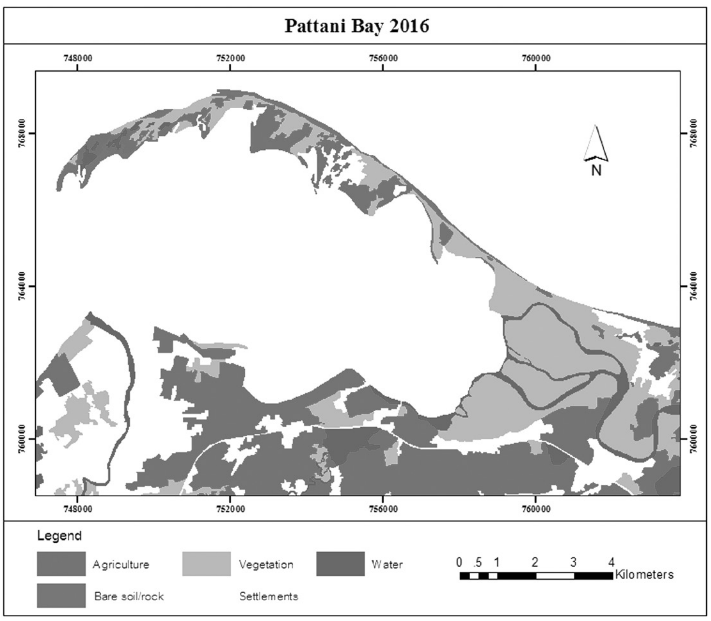


**Figure 12** Land Use Maps of Pattani Bay 2016

## Conclusion

After used ERDAS to perform the classification, significant data has been obtained using a Minimum Distance Supervised classification method. Correction methods need to be performed for shadows. Land use classification is more detailed using remote sensing tools such as ERDAS software than the ArcGIS. Also land use classification using ERDAS, can be performed faster and with more precision, after you have your training samples. Using the obtained results from ERDAS and ArcGIS for land use classification can help to perform a more accurate classification. To perform a better classification of this area using ERDAS, it is recommended to use the Modeler tool, to correct the errors and be more accurate.

## Acknowledgement

Comparison of Remote Sensing Techniques for Land Use Classification in Pattani Bay, Thailand has been given scholarship from National Research Council of Thailand (NRCT).

## References

Anderson, J.R., Hardy, E.E., Roach, J.T. & Witmer, R.E. (1976). **A Land Use and Land Cover Classification for Use with Remote Sensor Data.** Washington D.C.: U.S. Geological Survey.

Erftemeijer, P.L.A. & Bualuang, A. (2015). **Participation of Local Communities in Mangrove Forest Rehabilitation in Pattani Bay, Thailand**: Retrieved March 16, 2016, from http://www.globalrestorationnetwork.org/.

ESRI. (2016). **Introduction to ArcGIS.** CA: ESRI.

Grigg, D. (1965). The Logic of Regional Systems: Annals Assoc. Amer. **Geographers.** 55(3), 465-991.

Intergraph Corporation. (2013). **ERDAS Field Guide.** Huntsville, AL: Intergraph Corporation.

Jensen, J.R. (1996). **Introductory Digital Image Processing.** New Jersey: Prentice Hall, Inc.

Lillesand, T.M. & Kiefer, R.W. (2000). **Remote Sensing and Image Interpretation.** New York: John Wiley & Sons.

Lea, C. & Curtis, A.C., (2010). **Thematic Accuracy Assessment Procedures: National Park Service Vegetation Inventory, Version 2.0. Natural Resource Report NPS/2010/NRR-2010/204.** Colorado: National Park Service, Fort Collins.

Lu, D., Mausel, P., Brondízio, E. & Moran, E. (2004). Change Detection Techniques. **International Journal of Remote Sensing.** 25, 2365-2407.

Mallinis G., Emmanoloudis, D., Giannakopoulos, V., Maris, F. & Koutsias, N. (2011). Mapping and Interpreting Historical Land Cover/Land Use Changes in a Natura 2000 Site Using Earth Observational Data: The Case of Nestos Delta, Greece. **Applied Geography.** 31, 312-320.

NASA. (2017). **LANDSAT-8 Instruments.** Washington D.C.: U.S. NASA.

Ozesmi, S.L. & Bauer, M.E. (2002). Satellite Remote Sensing of Wetlands. **Wetlands Ecology and Management.** 10, 381-402.

Pavel, U. (2017). **Supervised Image Classification Using Minimum Distance Algorithm.** Ukraine: 50Northspatial.

Pirut, J. (2015). **Study on Community-Based Fishery Management: Case Study at Pattani Bay, Changwat Pattani.** University Library, Kasetsart University, Thailand.

Ruangchuay, R., Lueangthuwapranit, C. & Pianthumdee, N. (2007). Apparent Characteristics and Taxonomic Study of Macroalgae in Pattani Bay. **Songklanakarin Journal of Science and Technology.** 29(4), 893-905.

U.S. Geological Survey. (2017). **LANDSA- 8 (L-8) Data Users Handbook.** Washington D.C.: U.S. Geological Survey.

Zomeni M.J.T. & Pantis, J.D. (2008). Historical Analysis of Landscape Change Using Remote Sensing Techniques: An Explanatory Tool for Agricultural Transformation in Greek Rural Areas. **Landscape and Urban Planning.** 86, 38-46.